ICA69 IS A NOVEL RAB2 EFFECTOR REGULATING ER-GOLGI TRAFFICKING IN INSULINOMA CELLS*

Laura Buffa[1], Evelyn Fuchs[2], Massimo Pietropaolo[3], Francis Barr[2] and Michele Solimena[1,4,5]

[1]Experimental Diabetology and [4]Department of Medicine III, Carl Gustav Carus School of Medicine, Dresden University of Technology, Dresden 01307, Germany; [2]Cancer Research Centre, University of Liverpool, Liverpool L3 9TA; [3]Laboratory of Immunogenetics, The Brehm Center for Diabetes Research and Analysis, Department of Internal Medicine, University of Michigan Medical School, Ann Arbor, MI 48109, USA; [5]Max Planck Institute of Molecular Cell Biology and Genetics, Pfotenhauerstrasse 108, 01307 Dresden, Germany

Running title: ICA69, a Rab2 effector involved in early transport

Address correspondence to: Michele Solimena. Phone: +49 351 4586611; Fax: +49 351 4586330; E-Mail: michele.solimena@tu-dresden.de

Islet cell autoantigen of 69 kDa (ICA69) is a small GTPase binding protein of unknown function. ICA69 is enriched in the Golgi complex and its N-terminal half contains a BAR domain, a module that can bind/bend membranes and interacts with phospholipids. Here we show that in insulinoma INS-1 cells ICA69 binds to the small GTPase Rab2, which regulates the transport of COPI vesicles between the endoplasmic reticulum and the Golgi complex. Rab2 binds to ICA69 in a GTP-dependent fashion and recruits it to membranes. Over-expression of either Rab2 or ICA69 in INS-1 cells results in a phenotype characterized by: (i) redistribution of the coatomer subunit of COPI vesicles β-COP from membranes to the cytosol; (ii) impaired anterograde transport of the secretory granule protein precursors pro-ICA512 and chromogranin A; and (iii) reduction of stimulated insulin secretion. Taken together, these data identify ICA69 as a novel Rab2 effector and point to its role in regulating the early transport of insulin secretory granule proteins.

The presence of a BAR (Bin1, Amphiphysin and Rvs161/167) domain characterizes a large family of cytosolic proteins that are involved in membrane traffic in eukaryotic cells (1-3). The BAR domain confers the ability to impose a high curvature to the membrane lipid bilayer and/or to sense and bind the pre-existing highly curved membrane of transport vesicles (4-7). Proteins possessing a BAR domain include: the amphiphysins and endophilins, which are involved in endocytosis (8,9); the sorting nexins, which regulate the delivery of cargoes between endosomes and compartments in the biosynthetic and degradative pathways (10); and the arfaptins, which appear to inhibit protein transport from the ER to the Golgi complex (11). The presence of a BAR domain is also associated with the ability of many of these proteins to bind phospholipids (12), form homodimers and heterodimers with protein paralogues (13), and interact with various small GTPases, including ARF (14), Rac (15) and Rab proteins (16). Here we explore the function of a BAR domain-containing protein, Islet cell autoantigen of 69 kDa (ICA69), in the transport of insulinoma cells.

ICA69 is a protein of conserved homology and length (human: 483 aa; rat: 480aa; mouse: 478aa) (Fig. 1), whose N-terminal half encodes a BAR domain (3,17) and whose function is still unknown. ICA69 was originally identified by screening a pancreatic islet cDNA expression library with sera of pre-diabetic relatives of patients with type 1 diabetes (T1D) (18), which results from the autoimmune destruction of the insulin producing cells (β-cells) of the pancreatic islets. Autoantibodies directed against ICA69 have since been additionally identified in patients with rheumatoid arthritis and primary Sjögren's syndrome (19,20). As are most autoantigens of T1D, ICA69 is more abundant in neuroendocrine tissues, with peak levels in the brain and pancreatic islets (21). Additional studies suggested that a pool of ICA69 is membrane-bound (17,22) and enriched in the proximity of the Golgi complex. [^{32}P]GTP-blot overlay assays further

indicated that ICA69, similar to other proteins with a BAR domain, binds to a small GTP-binding protein of unknown identity (17). These data, together with the preferential autoimmune response in T1D towards secretory proteins and the inclusion of a BAR domain, strongly suggest that ICA69 is involved in vesicular transport.

Herein we demonstrate that ICA69 is a novel effector of Rab2 and that its over-expression inhibits anterograde transport in the early secretory pathway of the islet cell autoantigen 512 and chromogranin A, both markers of the insulin secretory granules.

MATERIALS AND METHODS

Two Hybrid screening – For yeast two-hybrid assays, Rabs were inserted into the bait vector pFBT9, pGBT9 (Clontech) modified to carry kanamycin resistance, while ICA69 and deletions thereof were inserted into the prey vector pACT2 (Clontech). Yeast two-hybrid assays were performed according to the yeast protocol handbook (Clontech), as described previously (23).

Cell culture - INS-1 cells were grown as previously described (24). For time-course stimulation, cells were pre-incubated for 1 h in resting buffer (0 mM glucose, 5 mM KCl) and then for 30 min in resting or stimulating (25 mM glucose, 55 mM KCl) buffers (25). Stimulated cells were thereafter incubated in resting buffer for 15, 30, 45, 60 or 90 min.

Transfection - INS-1 cells were transfected by electroporation with an Amaxa nucleofector as previously described (26) or a Laboratory Pulse Agile Electroporation System model PA-3,000 (Cytopulse Sciences). In the latter case cells were electroporated in the Cytoporation media kit (formula T; Cytopulse Sciences) with 4 pulses each at 580 Volts for 300 mseconds separated by a pause of 0.2 seconds. This series was repeated once after 1.5 min. For biochemical assays cells were transfected with 4 mg plasmid DNA, while for immunocytochemistry 1 mg plasmid DNA was used.

Insulin radioimmunoassay - Cell proteins were extracted in acid-ethanol (75% EtOH, 1.5% concentrated HCl, 23.5% H_2O) ON at -20 °C. The insulin content in cells and in medium (resting or stimulation buffer) was measured with the Sensitive Rat Insulin Radioimmunoassay (RIA) Kit (Linco Reseach). The insulin stimulation index (SI) was calculated as follows: *SI=Istim/(Istim+ICstim) vs. Irest/(Irest+ICrest)* where: I = secreted insulin medium (ng) and IC= cell insulin content (ng).

cDNA constructs - ICA69 cDNA was retro-transcribed from rat islets isolated as described (27) and cloned in pCRII-TOPO (Invitrogen). The ICA69 cDNA was then subcloned into pCDNA4/HisMAX-TOPO (Invitrogen) or pGEX-4T-1 (Amersham Biosciences) as XhoI-NotI insert in frame with GST. Human amphiphysin1 was subcloned from pcDNA3-HA-amphiphysin1 (a gift from P. De Camilli, Yale University, New Haven, USA) into pGEX-4T-1 as XbaI-BamHI insert in frame with GST. The cDNAs of human Rab2 fused to GFP and GST were gifts from F. Barr. The cDNAs of human Rab4, Rab5 and Rab6 fused to GST were gifts from M. Zerial (MPI-CBG, Dresden, Germany).

Immunocytochemistry - Cells grown on coverslips were fixed with 3% PFA in 120 mM Na-phosphate pH 7.4 for 20 min at 4 °C, washed once and incubated in quencing buffer (0.1 M glycine in PBS) for 20 min at room temperature (RT). After 5 washes cells were incubated in blocking solution GSDB (16.6% goat serum, 0.1% saponin, 20 mM Na-phosphate pH 7.4, 450 mM NaCl) for 45 min at RT and then immunostained in GSDB for 2 h at RT with the following primary antibodies: rabbit anti-ICA69 (18) (1:40); mouse anti-GM130 (BD Transduction Laboratories) (1:25); mouse anti-β-COP (clone maD; Sigma Chemical Co.) (1:50); rabbit anti-p58/ERGIC-53 (a gift from K. Svensson, Ludwig Institute for Cancer Research, Stockholm Branch, Karolinska Institutet, Stockholm, Sweeden) (28) (1:50). After washing, cells were incubated with anti-mouse or anti-rabbit Alexa488- or Alexa568-conjugated IgGs (Molecular Probes) for 1 h at RT, washed 5 times and mounted with ProLong Gold antifade reagent (Molecular Probes). Images were acquired with a Zeiss Axioverted 200 M confocal microscope (Carl Zeiss).

Cell extracts - Cells were washed with ice cold PBS and extracted in lysis buffer (10 mM Tris-HCl pH 8.0, 140 mM NaCl, 1% Triton X-100, 1mM EDTA, 1mM phenylmethylsulfonyl fluoride, 1% protease inhibitor cocktail (Sigma

Chemical)) for 30 min at 4 °C. For subcellular fractionation, 6 x 10^7 cells were resuspended in 1.5 ml homogenization buffer (0.32 M sucrose in 10 mM HEPES pH 7.5, 1% protease inhibitor cocktail). Cells were homogenized with 20 strokes in a ball-bearing homogenizer (H. Issel; ball of diameter 0.0016 inches, clearance 0.0012 inches). Cell homogenates were centrifuged at 3,000 x *g* for 10 min at 4 °C. 1 ml of the resulting post-nuclear supernatant was spun at 150,000 x *g* for 60 min at 4 °C. High-speed pellets were resuspended in 1 ml homogenization buffer. P1, P2 and cytosolic subcellular fractions were prepared as described (29). 6 x 10^7 cells were resuspended in 550 ml homogenization buffer, the P1 pellet in 100 ml and the P2 pellet in 60 ml of the same buffer. Protein concentration was assessed with the Bio-Rad Protein Assay Reagent (Bio-Rad Laboratories) or with the BCA™ protein assay kit (PIERCE Biotechnology).

Immunoprecipitation - Cells were washed with ice cold PBS and extracted in immunoprecipitation-lysis buffer (50 mM Tris-HCl pH 8.0, 150 mM NaCl, 1% Triton X-100, 1% protease inhibitor cocktail) for 30 min at 4 °C. For preclearing, 150 or 750 mg total protein were incubated for 1.5 h at 4 °C with 50 or 200 ml 50% ProteinG Sepharose beads (Amersham Biosciences), respectively. After centrifugation, supernatants were incubated overnight at 4 °C, and then for 2 h with ProteinG Sepharose. Beads were washed 5 times with washing buffer (50 mM Tris-HCl pH 7.4, 300 mM NaCl, 0.1% Triton X-100, 5 mM EDTA, 0.02% Na-azide) and once with PBS at 4 °C. Immunoprecipitates were eluted from the beads with SDS sample buffer and loaded on SDS-polyacrilamide gel.

Western blotting - Proteins were separated by 8-12% SDS-PAGE, transferred to nitrocellulose filters and immunoblotted with the following antibodies: rabbit anti-ICA69 (18) (1:500); mouse anti-ICA69 (17) (1:150); mouse anti-GM130 (1:250); goat anti-GFP (Protein Expression Facility, MPI-CBG, Dresden) (1:3,000); mouse anti-GFP (Clontech Laboratories) (1:1,000); rabbit anti-GST (Molecular Probes, Inc.) (1:2,000); mouse anti-□-tubulin (Sigma Chemical Co.) (1:5,000); mouse anti-Rabaptin4 (gift from M. Zerial) (1:1,000); mouse anti-EEA1 (BD Transduction Laboratories) (1:2,500); mouse anti-ICA512 (30) (1:75); mouse anti-CgA (BD Laboratories) (1:1,000). Protein signals were detected by chemiluminescence with the Supersignal West Pico Substrate or the Supersignal West Fempto Maximum Sensitivity Substrate (PIERCE Biotechnology) using a LAS-3000 Bioimaging System (Fuji) and quantified with the Image Gauge v3.45 software (Fuji).

GST pull down assay - GST fusion proteins were expressed in bacteria and GST pull-down assays were performed as previously described (31). 75 mg GST fusion protein or GST and 750 mg Triton X-100 soluble protein from INS-1 cells were used for each pull down assay. Pulled down proteins were analyzed by SDS-PAGE and western blotting.

Protein-lipid overlay assay - Phospolipid-spotted nitrocellulose membranes (PIP strips, Molecular Probes) were blocked with 3% Albumin fraction V in 10 mM Tris-HCl pH 8.0, 150 mM NaCl, 0.1% Tween-20. The membranes were incubated with 1 mg/ml GST, GST-ICA69 or GST-amphiphysin in blocking solution ON at 4 °C. The next day membranes were washed 3 times with blocking solution. Bound proteins were detected by western blotting.

Statistics and graphics - Statistical analyses were performed as previously described (26). Histograms were prepared with Microsoft Excel (Microsoft Corp.).

RESULTS

ICA69 is a novel Rab2-interacting protein – ICA69 was identified as a candidate effector protein for the activated (GTP) form of Rab2 in the context of a yeast two hybrid screening aimed at the identification of effector proteins for various Rab proteins (Table 1). Rab2 is a small GTPase that plays a role in ER-to-Golgi transport (32) and which is associated with the intermediate compartment (IC) (33). Previous studies suggested that Rab2 promotes the formation of COPI vesicles by recruiting the coatomer subunit of COPI vesicles, β-COP, to membranes (34). In the same screening ICA69 did not interact with any other Golgi or endosome localized Rabs tested.

ICA69 binds to Rab2-GTP through its BAR domain - To establish whether ICA69 interacts with Rab2 in mammalian cells, we performed immunoprecipitations with anti-GFP antibodies

from extracts of INS-1 cells transfected with either GFP-Rab2 or GFP as a negative control. Because a suitable Rab2 antibody could not be obtained, we relied on detection of GFP-Rab2 rather than endogenous Rab2 for all the experiments described here. Immunoprecipitates were separated by SDS-gel electrophoresis and immunoblotted with anti-ICA69 and anti-GFP antibodies (Fig. 2A). We found that ICA69 co-immunoprecipitated with GFP-Rab2 (lane 5), but not with GFP alone (lane 6), indicating ICA69 binds to Rab2.

To test whether ICA69 binding to Rab2 is nucleotide-dependent, we performed GST pull-down assays. Recombinant Rab2 fused to GST or GST alone were loaded either with GDP or GTPγS, and then incubated with Triton X-100 soluble extracts from INS-1 cells. Recovery of ICA69 with glutathione beads pre-loaded with GST-Rab2 or GST was then assayed by immunoblotting. We found that ICA69 was only pulled down from cell extracts by GST-Rab2 in its GTP-bound state (Fig. 2B, lane 4). GST-Rab2 bound to GDP (lane 3) and GST alone failed to pull down ICA69 (lane 2). Thus ICA69 interacts with Rab2 in a GTP-dependent fashion, fulfilling the criteria of a Rab2 effector (35).

To evaluate the specificity of ICA69 binding to Rab2, similar pull-down and immunoblot assays were performed with a number of different Rab proteins. We chose both Rab proteins with closely related location and function to Rab2, such as Rab1 and Rab6, and Rab proteins with more distantly related location/function, such as Rab4 and Rab5. Rab1 is known to be involved in anterograde membrane trafficking between the ER and the Golgi complex (32), while Rab6 is Golgi-associated and regulates both transport between early and late Golgi compartments and a Golgi-to-ER retrograde pathway that is COPI-independent (36). Rab4 has a role in sorting/recycling in early endosomes (37), while Rab5 is required for endosome fusion (35). We found that ICA69 was not pulled down by either Rab1, Rab4, Rab5 (Fig. 2C, upper panels) or Rab6 (data not shown), despite the proper folding and function of the first three mentioned Rabs as demonstrated by their ability to pull down their respective effectors, GM130, Rabaptin and EEA1, in a GTP-dependent fashion (Fig. 2C, lower panels). Considering the relative amount of each Rab effector in the input and on the beads following the pull-down assay, it appears that ICA69 binding to Rab2 is both strong and specific.

To identify the Rab2-binding domain of ICA69, we performed an additional yeast two hybrid screening (Table 2). This screen identified the N-terminal half of ICA69, mostly containing the BAR domain (Fig. 1), as the putative binding domain to Rab2.

Rab2 recruits ICA69 to membranes - Considering that ICA69 has been shown to partially associate with membranes (17), we further investigated the relationship of ICA69 and Rab2 by analyzing the subcellular distribution of both proteins in GFP-Rab2 transfected INS-1 cells. We first confirmed that GFP-Rab2 did not alter ICA69 expression levels compared to untransfected cells (Fig. 3A). Following subcellular fractionation of untransfected cells, ICA69 was mostly found in the high-speed supernatant (Fig. 3B and C), consistent with our previous data (17). Importantly, over-expression of GFP-Rab2 decreased the recovery of ICA69 in this fraction by 16±4.7% ($p=0.015$), while increasing it by 17±6.7% ($p=0.03$) in the particulate fraction, where GFP-Rab2 was also enriched (Fig. 3B, bottom panel). This indicates that Rab2 is able to alter ICA69 distribution by recruiting it to membranes. These results are particularly significant when the low efficiency of GFP-Rab2 transfection in INS-1 cells (~25%) is taken into account.

Additional evidence that Rab2 expression levels affect ICA69 distribution in INS-1 cells was obtained by confocal immunomicroscopy. In these cells we found that ICA69 associated with organelles distributed throughout the cytoplasm and was enriched in the perinuclear region, where it partially co-localized with the Golgi complex marker GM130 ((17) and Fig. 3D, panel a). In MDCK cells, Rab2 is associated with the IC in proximity to the perinuclear Golgi complex (33). Conversely, in INS-1 cells ICA69 and GFP-Rab2 largely co-localized on cytosolic organelles of pleiomorphic size and shape (Fig. 3D, panels b and c). Interestingly, in cells expressing the

highest GFP-Rab2 levels, in one or more large perinuclear structures (Fig. 3D, panel c, arrowheads). This pattern of ICA69 localization was rarely observed in untransfected cells or cells expressing low-to-moderate levels of GFP-Rab2.

To more accurately define the compartment where ICA69 interacts with Rab2, we performed co-localization studies using β-COP and ERGIC-53, a marker of the IC (28) (Fig. 4). In INS-1 cells, β-COP was associated with organelles that were distributed throughout the cytoplasm and contained no detectable GFP-Rab2 and ICA69. GFP-Rab2 also did not co-localize with ERGIC-53. Thus, the identity of the compartment where ICA69 and Rab2 interact remains to be determined.

Blocking ER-to-Golgi transport similarly perturbs localization of ICA69 and Rab2 - We investigated whether subcellular distribution of ICA69 and GFP-Rab2 is altered when membrane trafficking is disrupted early in the secretory pathway by BrefeldinA (BFA) treatment. BFA has been shown to inhibit guanine-nucleotide exchange on ARF1 (38) and causes redistribution of Golgi markers such as GM130 ((39) and Fig. 5A, compare panels a and b). INS-1 cells treated with BFA had far less detectable ICA69 (Fig. 5A, panels a-d) and GFP-Rab2 (Fig. 5A, panels c and d) than untreated cells. This decreased detection is consistent with redistribution of these proteins into the cytosol.

We next analyzed ICA69 and GFP-Rab2 distribution in INS-1 cells incubated at 15 °C, which enables better visualization of the IC by inhibiting anterograde ER-to-Golgi transport (28). At 37 °C, in cells expressing little to no GFP-Rab2, ICA69 was predominantly associated with pleiomorphic organelles scattered throughout the cytosol (Fig. 3D, panel b, arrows). In contrast, in cells expressing high levels of GFP-Rab2, ICA69 was concentrated in a few large GFP-Rab2 positive perinuclear structures (Fig. 3D, panel c and Fig. 5B, panel a, arrowheads). Notably, at 15 °C the predominant accumulation of ICA69 in a few large perinuclear structures was apparent regardless of GFP-Rab2 expression levels (Fig. 5B, panel b, arrows). Taken together, these data suggest that ICA69 is recruited to the IC in a Rab2-dependent fashion.

It is thought that low affinity binding of positively charged residues within BAR domains to phosphoinositides cooperate with small-GTPases to recruit BAR-containing proteins to membranes (2,4,40). To test whether ICA69 interacts with phosphoinositides, recombinant GST-ICA69 expressed in bacteria was purified and then used for overlay assays on membranes spotted with different phosphoinositides. Similar to another BAR domain-containing protein, GST-amphiphysin, but unlike GST alone, GST-ICA69 bound to several membrane lipids, and preferentially to phosphatidylinositol 4-phosphate (PI(4)P) (Fig. 6). *In vitro* binding of ICA69 to PI(4)P is consistent with its association with IC and Golgi elements, as increasing evidence points to an involvement of PI(4)P turnover in ER-to-Golgi membrane traffic (41).

ICA69 over-expression leads to redistribution of β-COP - To gain insight into the physiological role of ICA69, we analyzed the impact of its over-expression on various processes related to membrane trafficking in INS-1 cells. For these studies ICA69 was expressed as a fusion protein with an Xpress epitope and a poly-histidine tag at its C-terminus (ICA69-HisMAX, Fig. 7A). Previous *in vitro* studies indicated that Rab2 promotes the recruitment of the coatomer subunit β-COP to IC membranes in order to generate COPI vesicles (29,42). We found that although independent over-expression of GFP-Rab2 or ICA69-HisMAX in INS-1 cells did not affect the overall expression of β-COP (Fig. 7B), its membrane distribution was changed in a similar fashion with the over-expression of either Rab2 or ICA69. Specifically, their over-expression decreased the amount of β-COP in the P2 subcellular fraction, which mostly contains microvesicles, by 20±2.8% (GFP-Rab2; $p=0.08$) and 33±7.4% (ICA69-HisMAX; $p=0.014$) (Fig. 7C and D). In parallel, recovery of β-COP in the P1 fraction, which contains mainly ER, IC and Golgi membranes, was increased by 17±2.5% (GFP-Rab2; $p=0.04$) and 23±2.7% (ICA69-HisMAX; $p=0.02$). Following adjustment for levels of γ-tubulin, it appears that over-expression of ICA69-

HisMAX increased the levels of cytosolic β-COP by 43±8.9% (p=0.02). Redistribution of β-COP upon over-expression of ICA69 supports the involvement of the latter protein in early trafficking along the secretory pathway.

ICA69 over-expression impairs the early transport and release of granule proteins - Rab2 over-expression is know to correlate with a partial block in ER-Golgi trafficking (43). Thus we sought to determine whether ICA69 over-expression might also affect the early transport of secretory proteins. To this aim we analyzed the behavior of the precursors of islet cell autoantigen 512 (ICA512) (44) and chromogranin A (CgA) (45,46), two proteins of insulin-containing secretory granules. Pro-ICA512 is a glycoprotein of 110 kDa whose biosynthesis is stimulated by glucose. Upon arrival in the Trans Golgi Network (TGN) and sorting into secretory granules, its ectodomain is cleaved by a pro-hormone convertase. The resulting mature form of this protein has a molecular weight of ~65 kDa (ICA512-TMF) (25). CgA is synthesized as a polypeptide of 86 kDa that gives rise to various small peptides following its sorting into secretory granules and cleavage by protein convertases. Similarly to ICA512, its biosynthesis is rapidly induced by glucose (47).

To follow the maturation of pro-ICA512 and pro-CgA, control INS-1 cells and cells over-expressing GFP-Rab2 or ICA69-HisMAX were kept at rest for one hour, then glucose-stimulated for 30 min to enhance translation of granule proteins, and finally returned to resting medium for up to 60 min (Fig. 8A and B). In control cells, stimulation increased the levels of pro-ICA512 and pro-CgA (lane S), which then progressively decreased upon return to resting conditions because of their proteolytic conversion into their smaller, mature forms (lanes 15' to 60'), as shown in the case of ICA512. In contrast, in cells over-expressing GFP-Rab2 or ICA69-HisMAX, the levels of both pro-proteins were already up-regulated at resting conditions and their decay was significantly delayed relative to control cells. These data indicate that ICA69 over-expression, similar to Rab2 (29,43), impairs the maturation of pro-ICA512 and pro-CgA because of a partial block in the transport of secretory proteins along the early secretory pathway.

To investigate whether the delay of early transport of secretory proteins caused by Rab2 or ICA69 over-expression also has consequences for secretion, we measured insulin release. While the levels of insulin content did not significantly differ between untransfected and GFP-Rab2 or ICA69-HisMAX transfected INS-1 cells (Fig. 9A), over-expression of the latter proteins correlated with impaired insulin secretion by 28±5.2% (p=0.014) and 11±1.6% (p=0.006), respectively (Fig. 9B).

DISCUSSION

Several lines of evidence point towards a role for ICA69 in trafficking secretory proteins. The most suggestive indications are: a) ICA69 contains a BAR domain (17), a protein module that binds/bends membranes (4); and b) the original identification of ICA69 as a T1D autoantigen. A previous study from Pilon and coworkers (22) indicate that a *Caenorabditis elegans* lacking the ICA69 homologue *ric-19* (*C.elegans ric-19(pk690)*) has impaired acetylcholine neurosecretion as suggested by an increased sensitivity to aldicarb. However, we have shown that in insulinoma cells ICA69 is (17) enriched in the perinuclear region, in close proximity to markers of the Golgi complex, but it is not associated with synaptic-like microvesicles and mature insulin secretory granules (17). Thus, ICA69 is unlikely to be directly involved in neurosecretion. An impaired early transport of proteins required for regulated exocytosis may nevertheless account for the phenotype observed in *ric-19(pk690)* worms. We have previously reported that ICA69 interacts with a small GTP-binding protein (17). Here we demonstrate that ICA69 selectively binds Rab2 and begin to unravel the functional implications of this interaction.

Rab2 is a small GTPase that is involved in vesicle trafficking between the ER and the Golgi complex (43) and appears to be enriched in the IC (33). Over-expression of Rab2 (29), as well as Rab2 mutants that either fail to bind or hydrolyze GTP (32), has been shown to inhibit ER-to-Golgi

transport of vesicular stomatitis virus glycoprotein to different degrees. Rab2 also promotes recruitment of the β-COP subunit of the COPI vesicle coat to membrane (34). These findings led to the proposal that Rab2 plays a role in COPI-mediated vesicle formation (34) and participates, as does the COPI coat, in retrograde transport between the ER and Golgi complex (42). Additional evidence suggests that both Rab2 and COPI vesicles are also involved in anterograde transport along the secretory pathway (43,48-50). Despite significant efforts, however, the mechanism of Rab2 action in these cases remains unclear. There has been no data to support a direct interaction between Rab2 and β-COP, and no functional implications have been elucidated for the known Rab2 effectors, including glyceraldehyde-3-phosphate dehydrogenase (GAPDH) (51), one of the protein kinase C isoforms (PKCι/λ) (42), and the Golgi structural proteins GM130, GRASP55 and golgin-45 (52).

Here we discovered that Rab2 interacts with ICA69 by using a variety of assays, including pull-down with recombinant Rab2-GTPγS and immunoprecipitation. ICA69 immunoprecipitation with Rab2 initially suggested that this interaction might not be GTP-dependent, since the hydrolytic activity of a small GTPase is presumed to hydrolyze all bound GTP into GDP during the course of the immunoprecipitation experiment. However, our additional finding that ICA69 binds recombinant Rab2-GTPγS, but not Rab2-GDP, strongly argues that ICA69 is a Rab2-effector. Consistent with this, other Rab effectors have been shown to co-immunoprecipitate with their respective Rab, such as GAPDH with Rab2 (51) and Rabaptin4 with Rab4 (53). It should also be taken into account that the hydrolytic activity of Rab proteins varies. Rab2 in particular has such slow hydrolytic activity that most of it could conceivably remain in a GTP-bound state during the immunoprecipitation procedure (F. Barr, unpublished data). Moreover, it cannot be excluded that ICA69 binding further decreases Rab2 GTPase activity.

The close relationship of ICA69 with Rab2 was independently confirmed by imaging studies; we revealed that these two proteins extensively co-localize in particulate structures throughout the cytoplasm and redistribute together in INS-1 cells upon BFA treatment or incubation at 15 °C. Moreover, we observed that high levels of Rab2 are associated with the enrichment of ICA69 in large Rab2-containing perinuclear structures. Using subcellular fractionation assays of cells over-expressing Rab2, we clearly showed that Rab2 not only co-localizes with ICA69, but recruits it to membranes.

The fact that ICA69 interacts with membranes is further corroborated by our finding that it is able to bind to a large spectrum of phophoinositides, including PI(3)P, PI(4)P, PI(5)P, PI(3,4)P_2, PI(3,5)P_2, PI(4,5)P_2, and PI(3,4,5)P_3, in a protein-lipid overlay assay. Despite the limits of this approach and the overall weakness of ICA69 binding with different phosphoinositides, it is intriguing that ICA69 interacts preferentially with PI(4)P, which is required for vesicle budding from the Golgi complex (54). Overall, these data strongly suggest that ICA69 and Rab2 are in a complex on perinuclear structures that are spatially, and presumably functionally contiguous with the Golgi complex. The enlargement of these structures following the 15 °C block, suggests, but does not conclusively prove, that they belong to the IC.

In this study we address the functional role of ICA69, particularly in relation to Rab2. Despite multiple approaches, down-regulating ICA69 by RNA interference was unsuccessful (data not shown). Thus we analyzed the effect of over-expression on several aspects of membrane trafficking in INS-1 cells, including β-COP distribution, early transport of granule proteins and insulin secretion. We found that in all cases, over-expression of either ICA69 or Rab2 generates similar phenotypes. β-COP distribution changes in over-expressing cells such that it increasingly associates with membranes deriving from the ER, the IC and the Golgi complex, and decreasingly associates with small vesicles. In the case of ICA69 over-expression, the levels of cytosolic β-COP also increase. Notably, neither ICA69 nor Rab2 were found to colocalize with β-COP. How ICA69 and Rab2 interact with COPI vesicles in insulinoma cells remains uncertain. It does appear clear, however, that ICA69 and Rab2 play a role in

early transport as we found that their over-expression delays the maturation of granule protein precursors pro-ICA512 and pro-CgA. A delayed transport of newly synthesized granule components is likely to slow granule biogenesis, and thus may explain the reduced insulin secretion from ICA69 and Rab2 over-expressing INS-1 cells.

In the case of arfaptins, APPL-1 and APPL-2, the N-terminal BAR domain is known to mediate interactions with small GTPases. Likewise, we found that this domain is responsible for ICA69 binding to Rab2. Another feature of BAR domains is their ability to mediate homodimerization; however, we repeatedly did not recover homodimers between endogenous ICA69 and transfected ICA69-HisMAX from INS-1 cell extracts (data not shown). This may have been due to the fact that dimerization of BAR domain-containing proteins might require binding to membranes (54). Nevertheless, ICA69 dimers were not recovered even upon Rab2 over-expression, which promotes the recruitment of ICA69 to membrane. These issues issues may be fully addressed in the future by resolving the crystal structure of ICA69 alone and in complex with Rab2.

In conclusion, our results conclusively identify ICA69 as a novel effector of Rab2 and point to their related function in the early transport of insulin secretory granule proteins. Future studies on the Rab2-ICA69 complex may provide insight into the biogenesis of secretory vesicles.

REFERENCES

1.McMahon, H. T., and Gallop, J. L. (2005) *Nature* **438**(7068), 590-596
2.Itoh, T., and De Camilli, P. (2006) *Biochim Biophys Acta* **1761**(8), 897-912
3.Habermann, B. (2004) *EMBO Rep* **5**(3), 250-255
4.Peter, B. J., Kent, H. M., Mills, I. G., Vallis, Y., Butler, P. J., Evans, P. R., and McMahon, H. T. (2004) *Science* **303**(5657), 495-499
5.Takei, K., Slepnev, V. I., Haucke, V., and De Camilli, P. (1999) *Nature cell biology* **1**(1), 33-39
6.Bigay, J., Gounon, P., Robineau, S., and Antonny, B. (2003) *Nature* **426**(6966), 563-566
7.Blood, P. D., and Voth, G. A. (2006) *Proc Natl Acad Sci U S A* **103**(41), 15068-15072
8.Shupliakov, O., Low, P., Grabs, D., Gad, H., Chen, H., David, C., Takei, K., De Camilli, P., and Brodin, L. (1997) *Science* **276**(5310), 259-263
9.Gad, H., Ringstad, N., Low, P., Kjaerulff, O., Gustafsson, J., Wenk, M., Di Paolo, G., Nemoto, Y., Crun, J., Ellisman, M. H., De Camilli, P., Shupliakov, O., and Brodin, L. (2000) *Neuron* **27**(2), 301-312
10.Carlton, J., Bujny, M., Peter, B. J., Oorschot, V. M., Rutherford, A., Mellor, H., Klumperman, J., McMahon, H. T., and Cullen, P. J. (2004) *Curr Biol* **14**(20), 1791-1800
11.Williger, B. T., Ostermann, J., and Exton, J. H. (1999) *FEBS letters* **443**(2), 197-200
12.Zimmerberg, J., and McLaughlin, S. (2004) *Curr Biol* **14**(6), R250-252
13.Gallop, J. L., and McMahon, H. T. (2005) *Biochemical Society symposium* (72), 223-231
14.Kanoh, H., Williger, B. T., and Exton, J. H. (1997) *J Biol Chem* **272**(9), 5421-5429
15.Tarricone, C., Xiao, B., Justin, N., Walker, P. A., Rittinger, K., Gamblin, S. J., and Smerdon, S. J. (2001) *Nature* **411**(6834), 215-219
16.Talarek, N., Balguerie, A., Aigle, M., and Durrens, P. (2005) *Cell biochemistry and function* **23**(4), 253-266
17.Spitzenberger, F., Pietropaolo, S., Verkade, P., Habermann, B., Lacas-Gervais, S., Mziaut, H., Pietropaolo, M., and Solimena, M. (2003) *J Biol Chem* **278**(28), 26166-26173
18.Pietropaolo, M., Castano, L., Babu, S., Buelow, R., Kuo, Y. L., Martin, S., Martin, A., Powers, A. C., Prochazka, M., Naggert, J., and et al. (1993) *J Clin Invest* **92**(1), 359-371

19.Martin, S., Kardorf, J., Schulte, B., Lampeter, E. F., Gries, F. A., Melchers, I., Wagner, R., Bertrams, J., Roep, B. O., and Pfutzner, A. (1995) *Diabetologia* **38**(3), 351-355
20.Winer, S., Astsaturov, I., Cheung, R., Tsui, H., Song, A., Gaedigk, R., Winer, D., Sampson, A., McKerlie, C., Bookman, A., and Dosch, H. M. (2002) *Lancet* **360**(9339), 1063-1069
21.Karges, W., Pietropaolo, M., Ackerley, C. A., and Dosch, H. M. (1996) *Diabetes* **45**(4), 513-521
22.Pilon, M., Peng, X. R., Spence, A. M., Plasterk, R. H., and Dosch, H. M. (2000) *Mol Biol Cell* **11**(10), 3277-3288
23.Fuchs, E., Short, B., and Barr, F. A. (2005) *Methods in enzymology* **403**, 607-618
24.Asfari, M., Janjic, D., Meda, P., Li, G., Halban, P. A., and Wollheim, C. B. (1992) *Endocrinology* **130**(1), 167-178
25.Ort, T., Voronov, S., Guo, J., Zawalich, K., Froehner, S. C., Zawalich, W., and Solimena, M. (2001) *Embo J* **20**(15), 4013-4023
26.Trajkovski, M., Mziaut, H., Altkruger, A., Ouwendijk, J., Knoch, K. P., Muller, S., and Solimena, M. (2004) *J Cell Biol* **167**(6), 1063-1074
27.Gotoh, M., Maki, T., Kiyoizumi, T., Satomi, S., and Monaco, A. P. (1985) *Transplantation* **40**(4), 437-438
28.Saraste, J., and Svensson, K. (1991) *J Cell Sci* **100 (Pt 3)**, 415-430
29.Tisdale, E. J. (1999) *Mol Biol Cell* **10**(6), 1837-1849
30.Hermel, J. M., Dirkx, R., Jr., and Solimena, M. (1999) *Eur J Neurosci* **11**(8), 2609-2620
31.Christoforidis, S., and Zerial, M. (2000) *Methods* **20**(4), 403-410
32.Tisdale, E. J., Bourne, J. R., Khosravi-Far, R., Der, C. J., and Balch, W. E. (1992) *J Cell Biol* **119**(4), 749-761
33.Chavrier, P., Parton, R. G., Hauri, H. P., Simons, K., and Zerial, M. (1990) *Cell* **62**(2), 317-329
34.Tisdale, E. J., and Jackson, M. R. (1998) *J Biol Chem* **273**(27), 17269-17277
35.Zerial, M., and McBride, H. (2001) *Nat Rev Mol Cell Biol* **2**(2), 107-117
36.White, J., Johannes, L., Mallard, F., Girod, A., Grill, S., Reinsch, S., Keller, P., Tzschaschel, B., Echard, A., Goud, B., and Stelzer, E. H. (1999) *J Cell Biol* **147**(4), 743-760
37.Van Der Sluijs, P., Hull, M., Zahraoui, A., Tavitian, A., Goud, B., and Mellman, I. (1991) *Proc Natl Acad Sci U S A* **88**(14), 6313-6317
38.Klausner, R. D., Donaldson, J. G., and Lippincott-Schwartz, J. (1992) *J Cell Biol* **116**(5), 1071-1080
39.Yoshimura, S., Yamamoto, A., Misumi, Y., Sohda, M., Barr, F. A., Fujii, G., Shakoori, A., Ohno, H., Mihara, K., and Nakamura, N. (2004) *Journal of biochemistry* **135**(2), 201-216
40.De Matteis, M. A., Di Campli, A., and Godi, A. (2005) *Biochim Biophys Acta* **1744**(3), 396-405
41.Waugh, M. G., Minogue, S., Anderson, J. S., Balinger, A., Blumenkrantz, D., Calnan, D. P., Cramer, R., and Hsuan, J. J. (2003) *Biochem J* **373**(Pt 1), 57-63
42.Tisdale, E. J. (2000) *Traffic* **1**(9), 702-712
43.Tisdale, E. J., and Balch, W. E. (1996) *J Biol Chem* **271**(46), 29372-29379
44.Solimena, M., Dirkx, R., Jr., Hermel, J. M., Pleasic-Williams, S., Shapiro, J. A., Caron, L., and Rabin, D. U. (1996) *Embo J* **15**(9), 2102-2114
45.Huttner, W. B., and Benedum, U. M. (1987) *Nature* **325**(6102), 305
46.Hutton, J. C., Davidson, H. W., and Peshavaria, M. (1987) *Nature* **325**(6107), 766
47.Guest, P. C., Rhodes, C. J., and Hutton, J. C. (1989) *Biochem J* **257**(2), 431-437
48.Lippincott-Schwartz, J., Roberts, T. H., and Hirschberg, K. (2000) *Annu Rev Cell Dev Biol* **16**, 557-589
49.Appenzeller-Herzog, C., and Hauri, H. P. (2006) *J Cell Sci* **119**(Pt 11), 2173-2183
50.Duden, R. (2003) *Mol Membr Biol* **20**(3), 197-207
51.Tisdale, E. J., Kelly, C., and Artalejo, C. R. (2004) *J Biol Chem* **279**(52), 54046-54052
52.Short, B., Preisinger, C., Korner, R., Kopajtich, R., Byron, O., and Barr, F. A. (2001) *J Cell Biol* **155**(6), 877-883
53.Nagelkerken, B., Van Anken, E., Van Raak, M., Gerez, L., Mohrmann, K., Van Uden, N., Holthuizen, J., Pelkmans, L., and Van Der Sluijs, P. (2000) *Biochem J* **346 Pt 3**, 593-601

54.Simonsen, A., Wurmser, A. E., Emr, S. D., and Stenmark, H. (2001) *Curr Opin Cell Biol* **13**(4), 485-492

*FOOTNOTES

We thank Marino Zerial for reagents and critical advice; Jakko Saraste for the anti-ERGIC-53 antibody; Anke Altkrüger for excellent technical assistance; Stephan Munschke for the insulin radioimmunoassay; Carsten Schnatwinkel for advice on pull-down assays; Pietro De Camilli and Ronald Dirkx for critically reading this manuscript, Laurel Rohde for its editing. This work was supported by a MedDrive grant from the Medical School at the Technical University (TU) Dresden to L. Buffa and grants from the Deutsche Forschung Gemeinschaft (SFB 655), the Juvenile Diabetes Research Foundation and the BMBF to M. Solimena.

Abbreviations used are: BAR, Bin1, Amphiphysin and Rvs161/167; ER, Endoplasmic Reticulum; ICA69, Islet cell autoantigen of 69 kDa; T1D, type 1 diabetes; RIA, Rat Insulin Radioimmunoassay; SI, stimulation index; RT, room temperature; ON, overnight; IC, intermediate compartment; BFA, BrefeldinA; ICA512, islet cell autoantigen 512; TGN, Trans Golgi Network; GAPDH, glyceraldehyde-3-phosphate dehydrogenase; PKC, protein kinase C; SD, standard deviation; SEM, standard error of the mean.

FIGURE LEGENDS

Table 1. Putative ICA69/Rab2 interaction. Using the yeast two hybrid assay, ICA69 was tested against a panel of human Golgi and endosome localized Rab GTPases containing point mutations to trap them in the activate (GTP), or inactive (GDP) forms as indicated in the table. Growth on selective medium was scored after 3 days; (-) indicates no growth, while (+++) indicates strong growth.

Table 2. Mapping of the Rab2-binding domain of ICA69. Using the yeast two hybrid assay, ICA69 deletion mutants (1-250 and 251-480) were tested against activated Rab2. Growth on selective medium was scored after 3 days; (-) indicates no growth while (+++) indicates strong growth.

Fig. 1. Domain structure of ICA69. The primary structure of rat ICA69 (aa 1-480) includes a BAR domain in the N-terminal region (aa 53-250).

Fig. 2. ICA69 interacts with Rab2-GTP. A) Immunoprecipitations from extracts of INS-1 cells transiently transfected with pEGFP-Rab2 or pEGFP-N1 were carried out with an anti-GFP antibody. Immunoprecipitates (IP) were western blotted (WB) with antibodies against GFP or ICA69. Lanes 1 and 2: GFP-Rab2 and ICA69 in the input, respectively. Lanes 3 and 5: IP from INS-1 over-expressing GFP-Rab2. Lanes 4 and 6: IP from INS-1 cells over-expressing GFP. B) Pull-down assay from extracts of INS-1 cells with GST (lane 2), GST-Rab2-GDP (lane 3) and GST-Rab2-GTPS (lane 4) followed by WB for ICA69. Lane 1: input (10% of the extracts used for the pull-down). C) Pull-down assays from extracts of INS-1 cells with GST, and Rab1-, Rab4- or Rab5-GST loaded either with GDP or GTPγS, followed by WB for ICA69 or Rab1 effector GM130, Rab4 effector Rabaptin, and Rab5 effector EEA1.

Fig. 3. Rab2-dependent ICA69 membrane recruitment. A) and B) Western blottings (WB) on post-nuclear supernatants (A), high speed supernatants (HSS) and high speed pellets (HSP) (B) from untransfected and GFP-Rab2 INS-1 cells with antibodies against ICA69, GFP and γ-tubulin. In B) short (3 min) and long

(11 min) exposures of the same immunoblot for ICA69 are shown. C) Quantification of three independent experiments as in B. White bars: INS-1 cells; black bars: GFP-Rab2 INS-1 cells. The signals for ICA69 were normalized against g-tubulin and equaled to 100% in untransfected cells. Error bars indicate the standard deviation (SD) in the case of untransfected INS-1 cells, and standard error of the mean (SEM) in the case of pGFP-Rab2 INS-1 cells. *: $p<0.05$. D) Confocal microscopy of untransfected (a) and GFP-Rab2 (pseudogreen; b-d) INS-1 cells. Cells were immunolabeled for ICA69 (pseudored; a-c) and GM130 (pseudogreen; a). Co-localization of ICA69 with GFP-Rab2 is indicated with arrows. Arrowheads point to the perinuclear structures where ICA69 accumulates in those cells most abundantly over-expressing GFP-Rab2. Scale bar: 5 □m.

Fig. 4. Distribution of ICA69, Rab2 and β-COP in INS-1 cells. Confocal microscopy of GFP-Rab2 (pseudogreen; a and c) and untransfected (b) INS-1 cells. Cells were immunolabeled for β-COP (pseudored; a and b), ICA69 (pseudored; b), and ERGIC-53 (pseudored; c). Scale bar: 5 mm.

Fig. 5. Distribution of ICA69 and Rab2 upon blocking ER-to-Golgi transport. A) Confocal microscopy of untransfected (a and b) and GFP-Rab2 (pseudogreen; c and d) INS-1 cells. Cells were untreated or treated with BFA, as indicated, and immunolabeled for ICA69 (pseudored; a-d) and GM130 (pseudogreen; a and b). B) Confocal microscopy of GFP-Rab2 (pseudogreen) INS-1 cells incubated at 37 °C (a) or 15 °C (b) and then immunolabeled for ICA69 (pseudored). Arrowheads in A and B point to perinuclear structures where ICA69 accumulates in those cells most abundantly over-expressing GFP-Rab2. Scale bar: 5 μm.

Fig. 6. ICA69 interacts with phosphoinositides. Overlay assays with GST, GST-ICA69 or GST-amphiphysin on nitrocellulose filters spotted with phosphoinositides (PIP strips). The phosphoinositides spotted at each position are indicated. The assay was repeated twice, with similar results.

Fig. 7. ICA69 over-expression alters the distribution of β-COP. A) Western blotting on extracts of untransfected or ICA69-HisMAX INS-1 cells with anti-ICA69 or anti-Xpress. B) Western blotting on post-nuclear supernatants from untransfected, GFP-Rab2, or ICA69-HisMAX INS-1 cells with antibodies against β-COP and g-tubulin. C) Western blottings on subcellular fractionations from not transfected, GFP-Rab2, or ICA69-HisMAX INS-1 cells with antibodies against β-COP, ICA69, GFP and g-tubulin. P1: fast sedimenting membranes, P2: slow sedimenting membranes, Cyt: cytosol. D) Quantification of three independent experiments as in C. White bars: INS-1 cells; grey bars: GFP-Rab2 INS-1 cells; black bars: ICA69-HisMAX INS-1 cells. The signals for β-COP were normalized against γ-tubulin and equaled to 100% in untransfected cells. Error bars indicate the SD in the case of untransfected INS-1 cells, and SEM in the case of GFP-Rab2 and ICA69-HisMAX INS-1 cells. *: $p<0.05$.

Fig. 8. ICA69 over-expression impairs the early transport of secretory proteins. A) and B) Western blottings on extracts from untransfected, GFP-Rab2, or ICA69-HisMAX INS-1 cells with antibodies against ICA-512, CgA and γ-tubulin. Cells were kept at rest (R) in resting medium for 1.5 h, or at rest for 1 h and stimulated with high glucose and high potassium for 30 min (S), or at rest for 1 h, stimulated for 30 min, and returned in resting medium for the time indicated, up to 90 min.

Fig. 9. ICA69 over-expression inhibits insulin secretion. A) Insulin content and B) stimulated insulin secretion of untransfected, GFP-Rab2 and ICA69-HisMAX INS-1 cells. White bars: untransfected INS-1 cells; grey bars: GFP-Rab2 INS-1 cells; black bars: ICA69-HisMAX INS-1 cells (ICA69). Error bars indicate the SD in the case of untransfected INS-1 cells, and SEM in the case of GFP-Rab2 and ICA69-HisMAX INS-1 cells. *: $p<0.05$, **: $p<0.01$.

Table 1

Pray: ICA69	
Bait	**Interaction**
Rab1Q67L (GTP)	-
Rab2 (wt)	++
Rab2S20N (GDP)	-
Rab2Q65L (GTP)	+++
Rab5Q79L (GTP)	-
Rab6Q72L (GTP)	-
Rab33bQ92L (GTP)	-

Table 2

Bait: Rab2Q65L (GTP)	
Pray	**Interaction**
ICA69	+++
ICA69 1-250	+++
ICA69 251-480	-

Figure 1

Figure 2

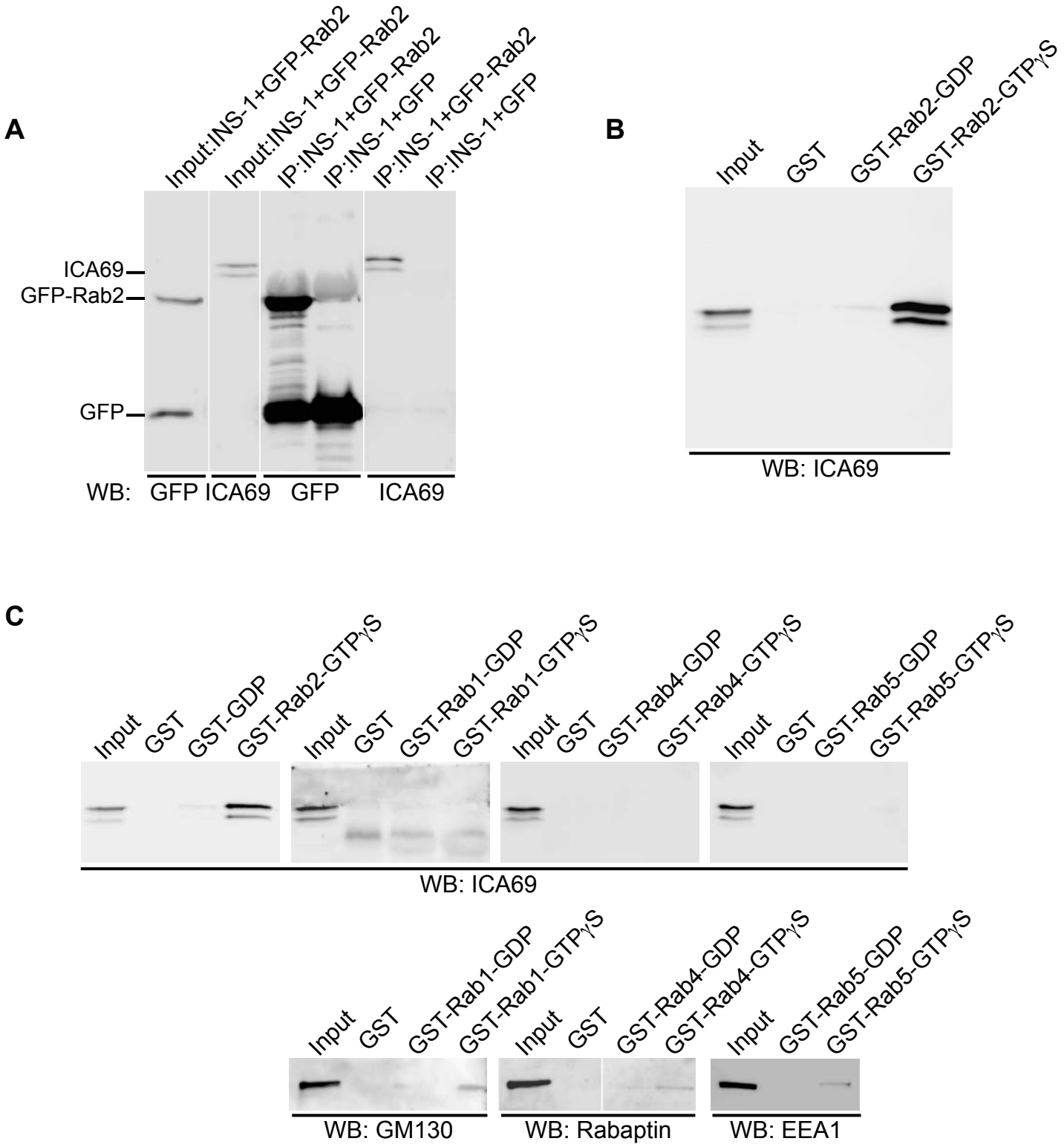
A
Input:INS-1+GFP-Rab2
Input:INS-1+GFP-Rab2
IP:INS-1+GFP-Rab2
IP:INS-1+GFP
IP:INS-1+GFP-Rab2
IP:INS-1+GFP
ICA69
GFP-Rab2
GFP
WB: GFP ICA69 GFP ICA69
B
Input
GST
GST-Rab2-GDP
GST-Rab2-GTPγS
WB: ICA69
C
Input
GST
GST-GDP
GST-Rab2-GTPγS
Input
GST
GST-Rab1-GDP
GST-Rab1-GTPγS
Input
GST
GST-Rab4-GDP
GST-Rab4-GTPγS
Input
GST
GST-Rab5-GDP
GST-Rab5-GTPγS
WB: ICA69
Input
GST
GST-Rab1-GDP
GST-Rab1-GTPγS
Input
GST
GST-Rab4-GDP
GST-Rab4-GTPγS
Input
GST-Rab5-GDP
GST-Rab5-GTPγS
WB: GM130
WB: Rabaptin
WB: EEA1

Figure 3

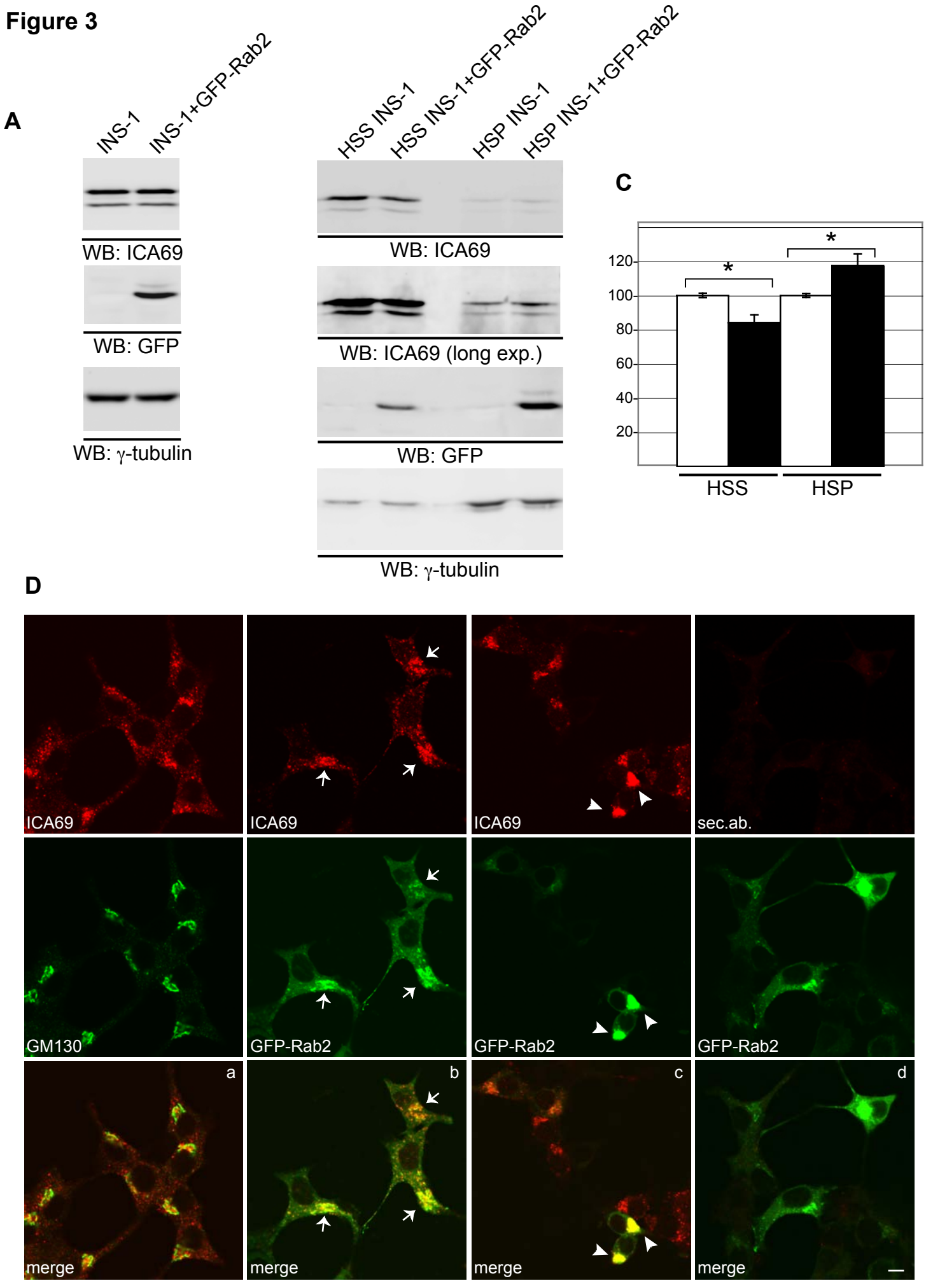
A
INS-1
INS-1+GFP-Rab2
WB: ICA69
WB: GFP
WB: γ-tubulin
HSS INS-1
HSS INS-1+GFP-Rab2
HSP INS-1
HSP INS-1+GFP-Rab2
WB: ICA69
WB: ICA69 (long exp.)
WB: GFP
WB: γ-tubulin
C
120
100
80
60
40
20
*
*
HSS
HSP
D
ICA69
ICA69
ICA69
sec.ab.
GM130
GFP-Rab2
GFP-Rab2
GFP-Rab2
a
b
c
d
merge
merge
merge
merge

Figure 4

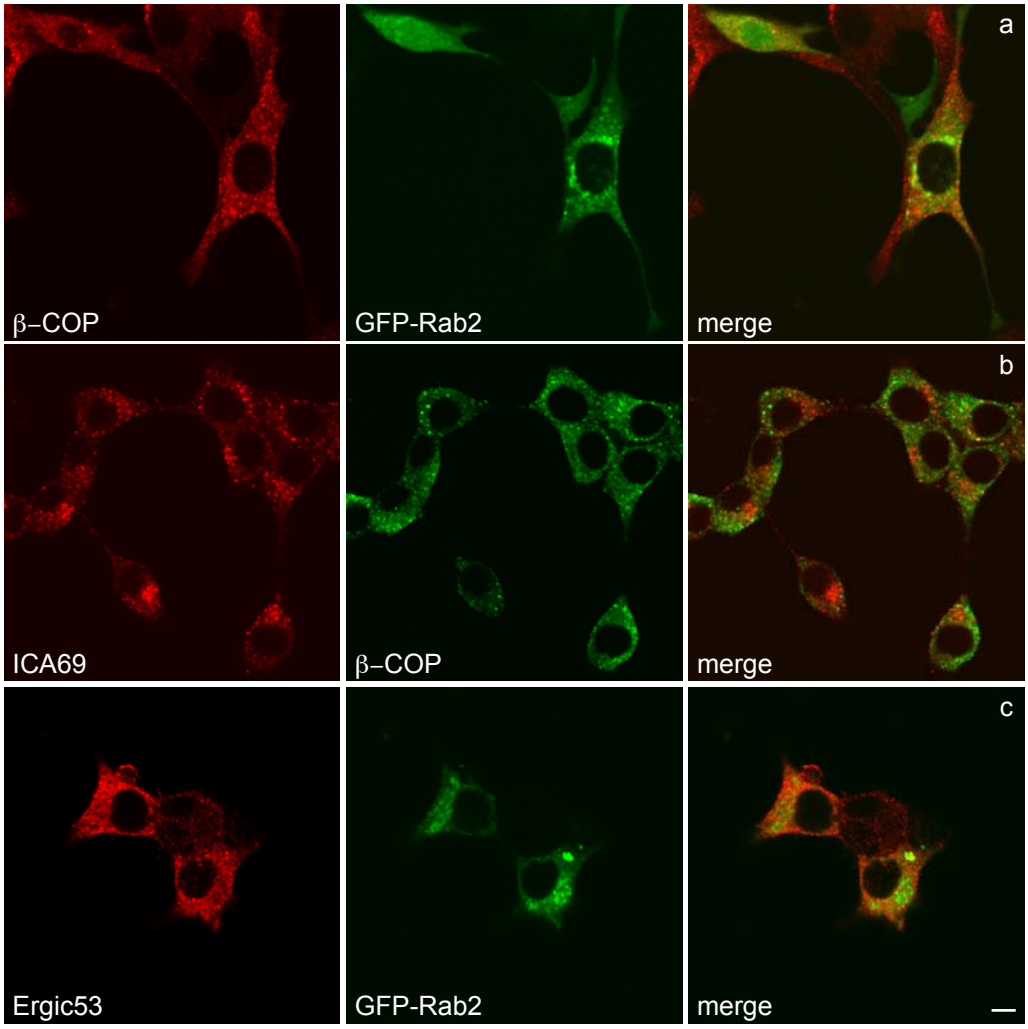
β–COP
GFP-Rab2
merge
a
ICA69
β–COP
merge
b
Ergic53
GFP-Rab2
merge
c

Figure 5

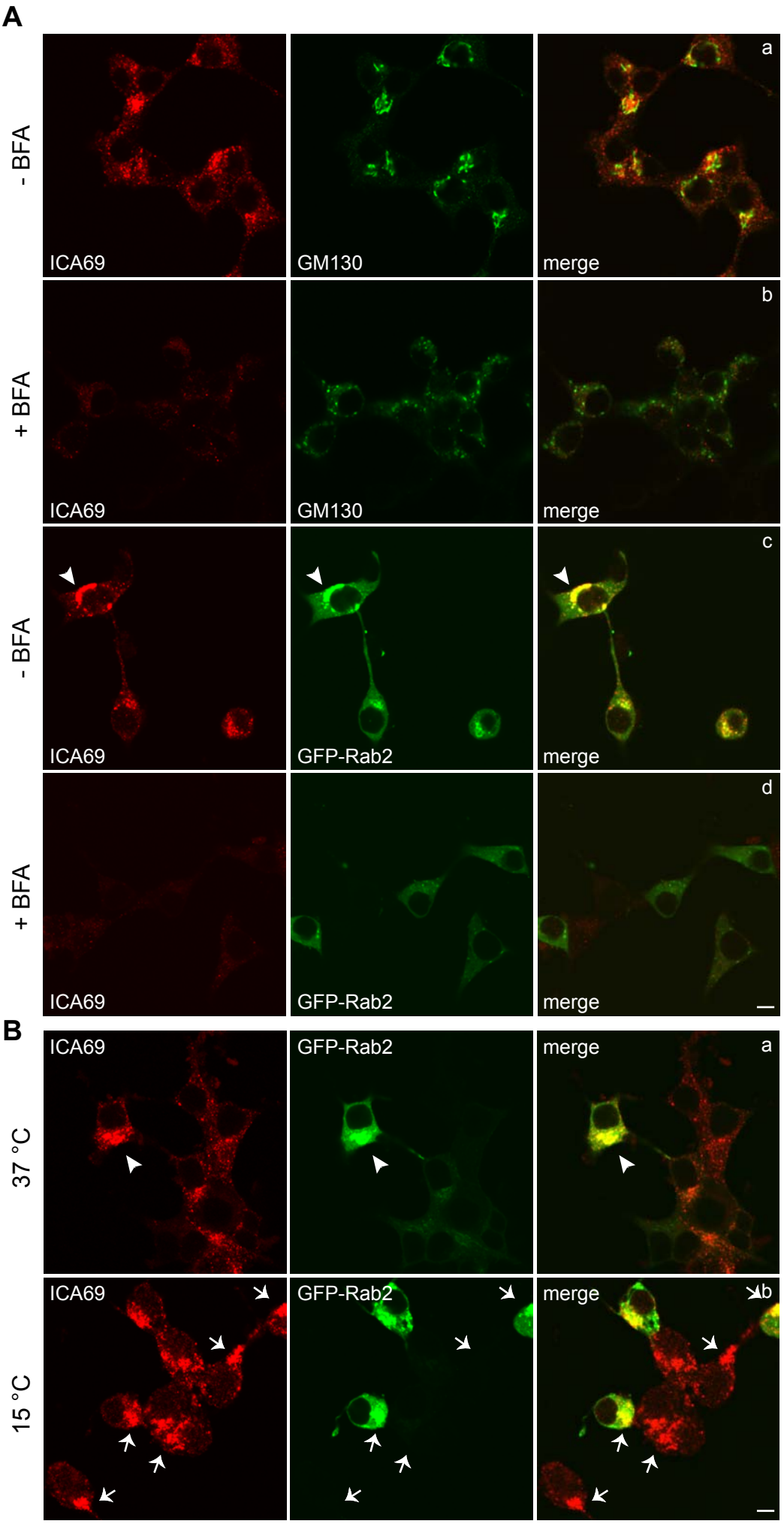
A
- BFA
+ BFA
- BFA
+ BFA
ICA69
GM130
merge
a
b
ICA69
GM130
merge
ICA69
GFP-Rab2
merge
c
ICA69
GFP-Rab2
merge
d
B
37 °C
15 °C
ICA69
GFP-Rab2
merge
a
ICA69
GFP-Rab2
merge
b

Figure 6

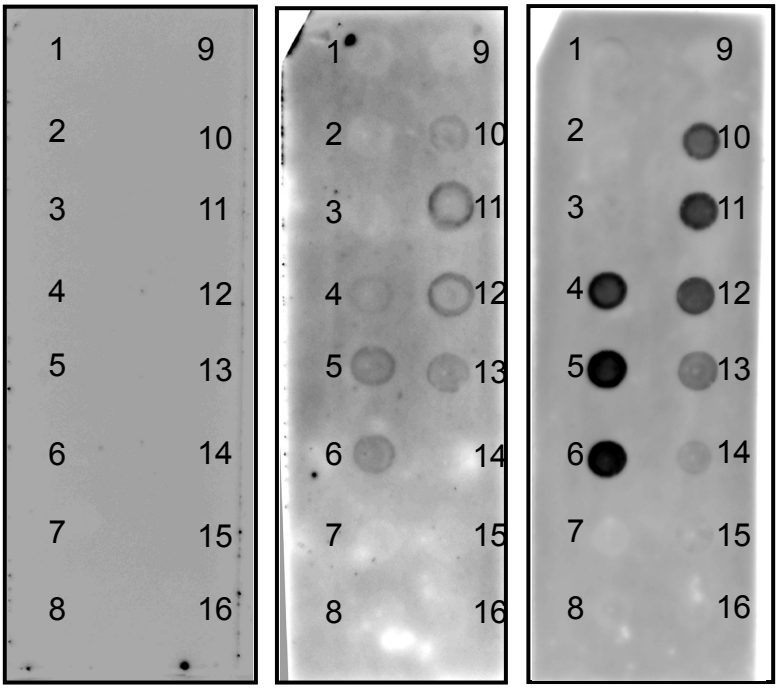

1.Lysosphosphatidic acid
2.Lysophosphatodylcholine
3.Phosphatidylinositol(PtdIns)
4.PtdIns(3)P
5.PtdIns(4)P
6.PtdIns(5)P
7.Phosphatidylethanolamine
8.Phosphatidylcholine
9.Sphingosine1-P
10.PtdIns(3,4)P2
11.PtdIns(3,5)P2
12.PtdIns(4,5)P2
13.PtdIns(3,4,5)P3
14.Phosphatidic acid
15.Phosphatidylserine
16.Blank

Figure 7

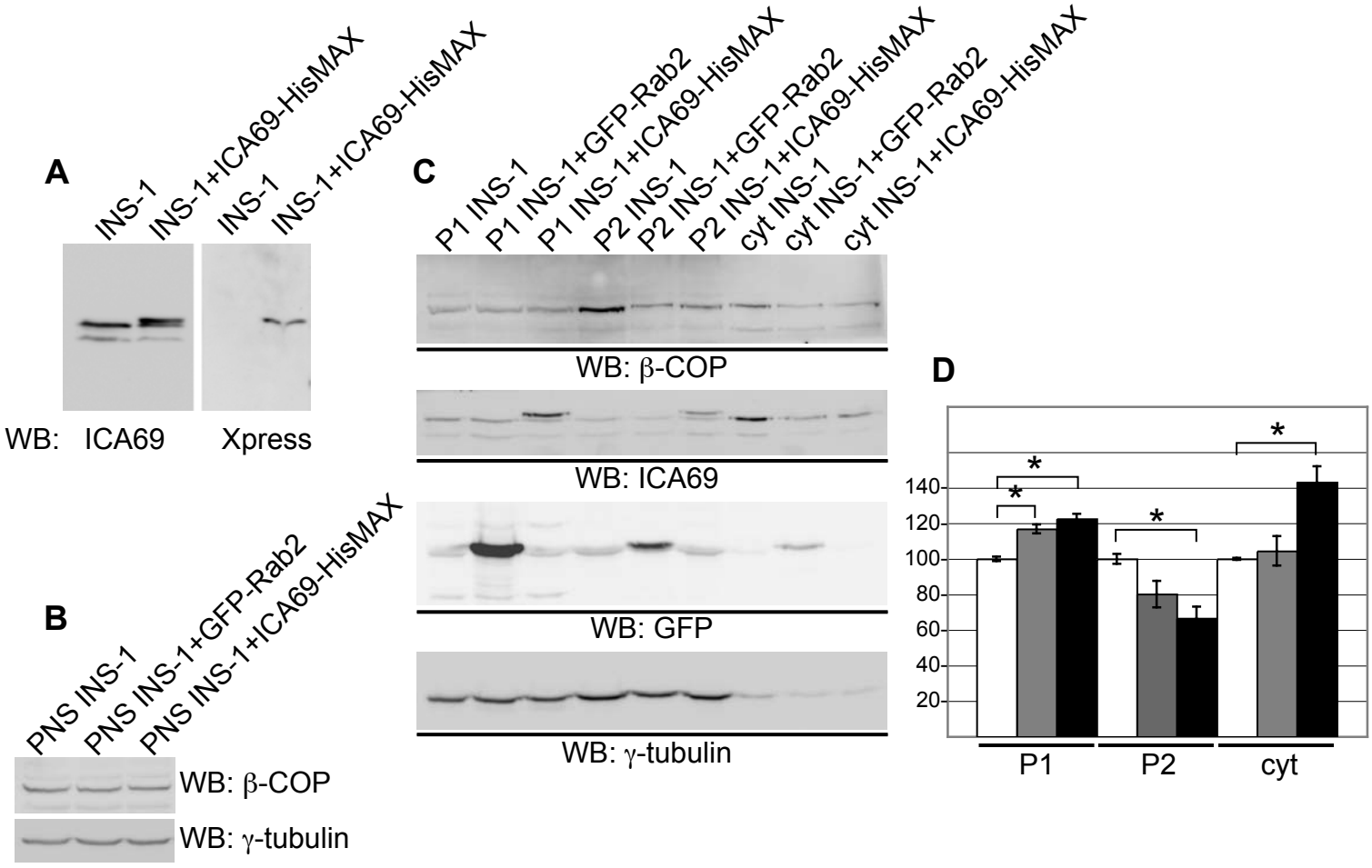
A
INS-1
INS-1+ICA69-HisMAX
INS-1
INS-1+ICA69-HisMAX
WB: ICA69
Xpress
B
PNS INS-1
PNS INS-1+GFP-Rab2
PNS INS-1+ICA69-HisMAX
WB: β-COP
WB: γ-tubulin
C
P1 INS-1
P1 INS-1+GFP-Rab2
P1 INS-1+ICA69-HisMAX
P2 INS-1
P2 INS-1+GFP-Rab2
P2 INS-1+ICA69-HisMAX
cyt INS-1
cyt INS-1+GFP-Rab2
cyt INS-1+ICA69-HisMAX
WB: β-COP
WB: ICA69
WB: GFP
WB: γ-tubulin
D
140
120
100
80
60
40
20
P1
P2
cyt

Figure 8

A

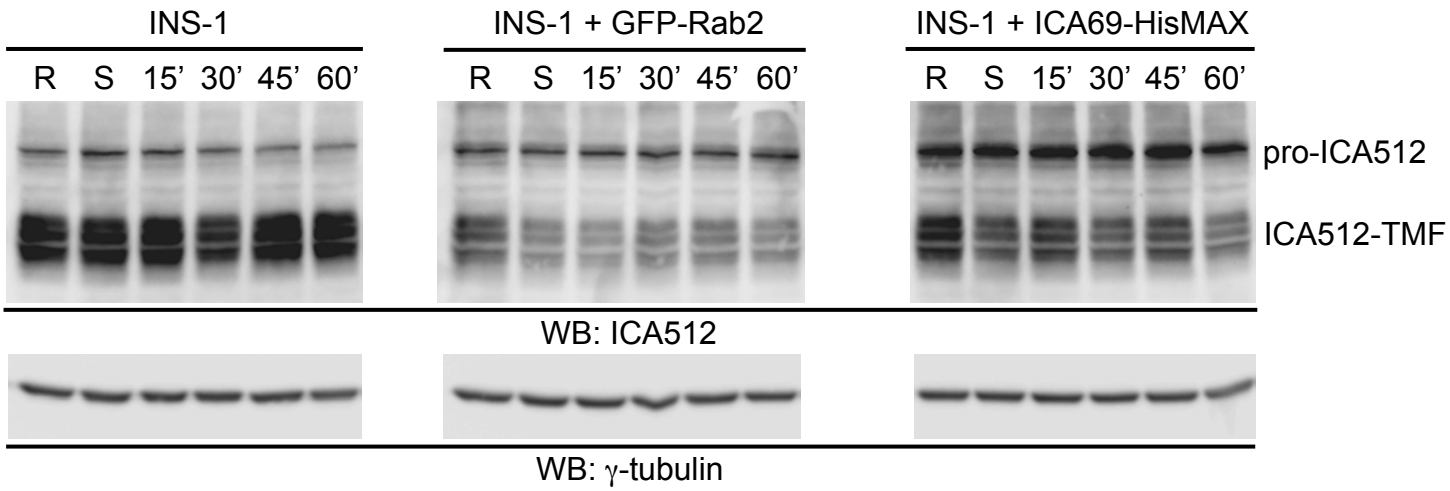
INS-1
INS-1 + GFP-Rab2
INS-1 + ICA69-HisMAX
R S 15' 30' 45' 60'
R S 15' 30' 45' 60'
R S 15' 30' 45' 60'
pro-ICA512
ICA512-TMF
WB: ICA512
WB: γ-tubulin

B

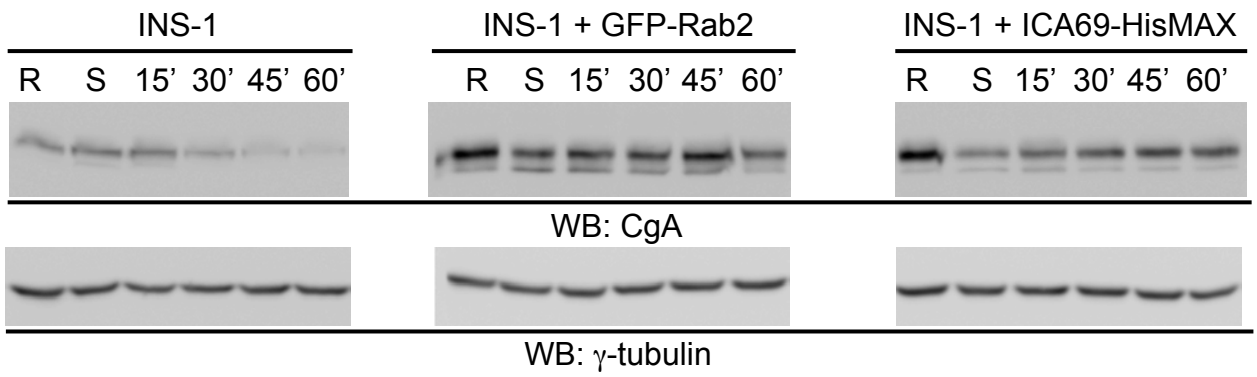
INS-1
INS-1 + GFP-Rab2
INS-1 + ICA69-HisMAX
R S 15' 30' 45' 60'
R S 15' 30' 45' 60'
R S 15' 30' 45' 60'
WB: CgA
WB: γ-tubulin

Figure 9

A

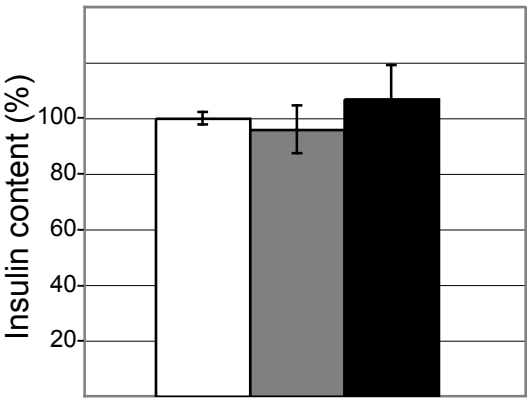

B